ANALYSING RAYLEIGH - BENARD - MARANGONI CONVECTION: 2D AND 3D FLUID SURFACES THROUGH MATHEMATICAL MODELLING

Kavitha Vanga[1,*] and Guddati Bala Chandra Mouli[2]

Received: June 19, 2025; Revised: May 19, 2026; Accepted: June 23, 2026

Abstract

Rayleigh-Bénard-Marangoni convection represents a complex interplay of buoyancy-driven, surface tension-induced, and density gradient effects in fluid systems. This review study uses mathematical modelling techniques to give an in-depth description of the Rayleigh-Bénard-Marangoni convection process, distinguishing between 2D and 3D fluid surfaces. The investigation delves into the distinctive characteristics of convection patterns and flow behaviours in these two-dimensional and three-dimensional domains. Through a comprehensive literature survey, this paper examines the fundamental mechanisms of each convection type and their interactions, elucidating the underlying physics and mathematical formalisms. The review highlights key mathematical models employed to simulate Rayleigh-Bénard-Marangoni convection, discussing their strengths and limitations in capturing the intricacies of each dimensionality. This work also addresses how several parameters, like the Rayleigh number, Marangoni number, and others, affect the observed convection processes. The findings offer valuable insights into the nuanced behaviour of convection processes on 2D and 3D fluid surfaces, providing a foundation for future research and engineering applications involving heat transfer, fluid dynamics, and materials processing.

Keywords: **Buoyancy-driven, Surface tension-induced, Density gradient, Rayleigh number, Marangoni number, Rayleigh-Bénard-Marangoni convection**

Introduction

Industrial engineering relies on fluid flow research because it helps enhance machine capabilities and boosts operational productivity (Rahman, 2024). Physics classes teach students about the essential subject of fluid dynamics, which studies how liquids and gases behave when they flow. Fluid dynamics studies how fluids behave when they move through space (Maharani *et al.*, 2024). Through modeling Fluid Dynamic (FD) challenges, scientists can apply their research methods to various fields including astrophysics, chemistry, environmental studies, civil engineering,

[1] *Department of Mathematics Vardhaman College of Engineering Kacharam(Village), Hyderabad, Telangana, 501218, India, E-mail: vkavithaou@gmail.com, ORCID: 0000-0002-2354-8138*
[2] *Department of Mathematics, Aditya College of Engineering & Technology, Surampalem 533437, Kakinada District, Andhra Pradesh, India, E-mail: gbchandramouli@gmail.com, ORCID: 0009-0006-0139-7339*
[*] *Corresponding author*

DOI: https://doi.org/10.55766/sujst10426

Suranaree J. Sci. Technol. 33(5):030416(1-15)

biomedical engineering, and mechanical engineering. The researchers aim to create simulations that will help them forecast results in various situations without needing to spend money on real-world tests during product development (Botarelli *et al.*, 2025). Rayleigh-Bénard convection (RBC) provides researchers with a fundamental natural thermal convection system that demonstrates how fluid flow patterns develop when heat rises from a heated surface to a cooler one between two horizontal structural elements (Saini *et al.*, 2025).

Surface tension forces at the fluid-fluid boundary arise from the molecular cohesive forces that exist between different liquid molecules. Surface tension exists as a stable value throughout the entire interface, or it exhibits variations because of temperature differences, concentration changes, and non-uniform surfactant distribution at the boundary surface. The temperature gradient causes the molten pool to have different surface tension, which produces a flow pattern that improves heat transfer throughout the entire volume, and this effect shows how the molten area develops its final shape and size. The Marangoni effect describes the flow pattern that results from differential surface tension between two surfaces (Bombe *et al.*, 2024). Marangoni convection stands as the second most crucial mechanism for transferring heat and mass between surfaces, since it results from surface tension differences at their contact points. The interface between two substances experiences this effect, which depends on three factors: temperature, solute concentration, and surfactant presence at the interface (Umavathi *et al.*, 2025). The combination of buoyancy with Marangoni effects creates a new hybrid mechanism that scientists name Rayleigh-Bénard–Marangoni (RBM) convection, because it produces more intricate patterns than each individual effect. Recent 3D numerical simulations of Bénard–Marangoni convection in open cavities with low Prandtl number fluids have demonstrated that increasing Marangoni number leads to two flow pattern bifurcations together with changes in heat and mass transfer properties, which demonstrates how surface tension interacts with thermal forces to create complex flow patterns (Jiang *et al.*, 2024). The study of RBM convection in layered systems and liquid metal environments shows that multi-physics interaction needs to be studied, because it determines how convective plumes and interfacial dynamics affect transport phenomena (Jiang *et al.*, 2024). The Rayleigh-Bénard-Marangoni system exhibits formation of convective cells through buoyancy-driven convection, which occurs because of the vertical temperature gradient. The temperature differences together with surface tension gradients create the Marangoni effect, which causes surface tension variations at the fluid interface to generate flow. The Marangoni effect creates extra challenges for fluid dynamics because it enables temperature-dependent surface tension changes to affect flow behavior, which differs from standard Rayleigh-Bénard convection that maintains constant fluid properties at its free surface (Sari *et al.*, 2024).

Traditional research on Rayleigh-Bénard and Marangoni convection utilizes simplified single-layer and two-dimensional fluid models which do not accurately simulate actual physical systems. The majority of established research uses linear stability theory which prevents researchers from studying complete nonlinear behavior and advanced convection patterns. Researchers typically examine the combined effects of buoyancy and surface tension and density-driven mechanisms as separate entities instead of using a unified hybrid approach. The complexity of multilayer fluids together with the instability problems of three-dimensional geometries creates computational obstacles for many numerical methods.

The accurate prediction of critical instability parameters together with transition conditions remains challenging when thermal and interfacial forces interact with each other. The existing limitations of the current system need more powerful computational methods together with detailed modeling techniques to handle the required complex tasks. The present study presents a unified mathematical framework which enables the analysis of hybrid Rayleigh-Bénard-Marangoni convection in two-dimensional and three-dimensional fluid systems through advanced finite element techniques.

The main contribution of the work is enumerated as:

- Established a complete mathematical system for investigating hybrid Rayleigh-Bénard-Marangoni convection in multilayer fluid systems, which function through combined thermos-capillary and buoyancy effects.
- Performed a dimensional analysis to investigate how convection patterns differed between two-dimensional and three-dimensional spatial arrangements.
- Created a fast numerical system which combines the Least Squares Finite Element Method (LSFEM) with Newton linearization and adaptive time-stepping to solve nonlinear governing equations.
- Numerical methods are used to find critical instability points while studying convection development to examine how Rayleigh and

Marangoni numbers affect flow patterns and thermal transport processes.

Literature Survey

Researchers have conducted extensive investigations on fluid convection mechanisms which include Rayleigh-Bénard and Marangoni convection because these mechanisms play crucial roles in heat transfer and fluid dynamics applications. Researchers used linear stability analysis together with two-dimensional simplified models to study how instability begins and how flow patterns develop through their studies. The basic insights from these methods showed their shortcomings because they could not handle nonlinear interactions and multilayer setups as well as mixed hybrid effects. This section reviews the existing theoretical and numerical studies on hybrid Rayleigh-Bénard-Marangoni convection and identifies the research gaps motivating the present work.

Dubey *et al.* (2025) proposed a theoretical and numerical investigation of Rayleigh-Bénard-Marangoni convection in binary fluid systems, focusing on the influence of fluid miscibility on the onset of oscillatory instability modes. The study used a phase-field formulation with linear stability analysis to track how stationary convection patterns changed into oscillatory convection patterns at different levels of miscibility. The results showed that partial miscibility created a critical Rayleigh number and Marangoni number threshold which determined when instability began. The analysis focused on linear stability tools and idealized setups which restricted its capacity to observe all nonlinear convection patterns together with intricate three-dimensional flow movements.

Schindler *et al.* (2025) conducted an experimental and numerical study to examine how fluid flow impacts thermal boundary-layer behavior in turbulent liquid-metal Rayleigh-Bénard convection. The study examined how heat transfer properties and boundary layer thickness changed with different Rayleigh number levels while studying how turbulent flow patterns affected thermal energy movement through the system. The experimentation revealed that fluid flow patterns brought about better boundary layer stability while increasing heat transfer efficiency throughout low-Prandtl-number liquid metal systems. The research focused exclusively on turbulent single-layer liquid metal systems and failed to examine either hybrid thermocapillary effects or multilayer convection interactions.

Song *et al.* (2024) used direct numerical simulation to study rapidly rotating Rayleigh-Bénard convection at high Rayleigh numbers so they could examine how buoyancy and Coriolis forces affect flow patterns. The study examined how heat transfer patterns developed, how flow patterns emerged, and how boundary layer development occurred under strong rotational movements. The findings showed that rapid rotation altered both plume development and convection flow patterns through its impact on system operations. The research focused exclusively on single-layer buoyancy-driven systems while excluding both surface tension-driven effects and hybrid Rayleigh-Bénard-Marangoni interactions from its examination.

Elbousefi *et al.* (2025) conducted a numerical study which analyzed Marangoni convection behavior in self-rewetting fluid layers that contained a flexible interface within a square enclosure which received uneven heat distribution. The research study analyzed how interface deformation and thermocapillary stresses and thermal gradients affected both flow patterns and heat transfer performance. The research findings showed that nonuniform heating created significant changes which affected interstitial movement patterns and helped create thermocapillary-driven circulation throughout the enclosure space. The research study only examined convection which depended on surface tension because it did not include buoyancy-driven convection or hybrid Rayleigh-Bénard-Marangoni interactions in multilayer systems.

Yan *et al.* (2025) proposed a phase-field numerical simulation to investigate the thermocapillary migration of a self-rewetting droplet on an inclined surface under imposed thermal gradients. The study examined droplet behavior by testing three different factors which included inclination angle along with surface tension changes and temperature distribution. The results showed that thermocapillary stresses controlled both droplet shape changes and movement direction toward the heated surface. The research study only examined the behavior of a single droplet while it omitted both buoyancy-driven convection and large-scale hybrid Rayleigh-Bénard-Marangoni interactions which occur in multilayer fluid systems.

Veena and Siddheshwar (2024) assessed Rayleigh-Bénard-Marangoni convection stability through energy stability analysis in both homogeneous and heterogeneous nanoliquid systems to identify the thresholds that lead to

convection instability. The research developed a mathematical framework that included nanoparticle effects to assess stability boundaries through energy method analysis. The study found that stability characteristics under two testing conditions showed different results between homogeneous and heterogeneous nanoliquid systems. The research results remained theoretical because they only investigated stability limits without studying nonlinear flow behavior or hybrid convection systems through three-dimensional computational analysis.

Waris *et al.* (2024) conducted a thermographic study about Marangoni-Rayleigh-Bénard convection which occurs in fluids whose temperature-dependent physical properties control surface topography. The research investigated how surface topography and changing thermophysical properties affected convection patterns and heat transfer processes during combined buoyancy and thermocapillary effects. Their results demonstrated that temperature-dependent properties significantly modified flow structures and instability characteristics in the coupled convection system. The analysis concentrated on controlled geometric environments while it did not investigate multilayer fluid systems or detailed three-dimensional nonlinear computational modeling of hybrid convection dynamics.

Liapidevskii (2024) created a two-layer equilibrium model which simulates how miscible inhomogeneous fluids flow when they encounter stratified conditions. The study developed a mathematical formulation which enabled researchers to study equilibrium states and flow characteristics by considering density changes and interlayer connections. The results provided analytical insights into the stability and structural behaviour of layered miscible fluid systems. The model concentrated on equilibrium configurations while omitting thermocapillary effects and buoyancy-driven instability initiation and nonlinear hybrid Rayleigh-Bénard-Marangoni convection behavior.

Verma *et al.* (2024) proposed an investigation into the interplay between light momentum transfer and fluid mechanical behaviour in two-layer liquid systems. The study developed a theoretical and computational framework to examine how optical forces affected interfacial dynamics and flow patterns in stratified fluids. The results demonstrated that radiation pressure and optical momentum significantly altered interface deformation and induced fluid motion in layered configurations. The analysis examined only optically driven flow mechanisms while excluding both buoyancy-driven and thermocapillary-driven instability mechanisms of hybrid Rayleigh-Bénard-Marangoni convection systems.

Huang *et al.* (2024) conducted an experimental study which examined how interface coupling interacted with multiple Faraday instability mechanisms in a three-layer fluid system which received periodic external stimulation. The study developed a theoretical and numerical framework to analyse wave interactions, interfacial coupling mechanisms, and the emergence of multiple instability modes. The study found that strong interface coupling created major effects on mode selection which resulted in different critical conditions needed for instability to start in stratified fluids. The study only examined vibration-induced Faraday instabilities while it excluded both buoyancy-driven and thermocapillary convection effects.

Costa *et al.* (2025) used computational fluid dynamics (CFD) to analyze how multi-layer cooling channels in three-dimensional grinding wheels affected fluid flow and thermal performance. The study used numerical methods to study how coolant distribution and heat dissipation efficiency and pressure drop behavior changed in layered channel geometries. The results showed that optimized multi-layer channel configurations improved cooling effectiveness together with better thermal management of grinding applications. The investigation focused on one specific application because it studied only particular operating conditions while omitting both nonlinear flow instabilities and general multilayer fluid interaction dynamics.

Wang *et al.* (2023) developed a study which examined how thermal convection heat transfer and flow patterns operate between two liquid layers by studying interfacial interactions and their convective properties. The researchers used numerical simulations to study how temperature and velocity and heat transfer properties behaved in fluid layers which had different density levels. The study results showed that interfacial coupling created a major impact on how flow patterns developed and it also changed the total efficiency of heat transfer throughout the system. The research investigation focused on buoyancy-driven thermal convection while excluding both thermocapillary effects and the complete range of hybrid convection methods which interact with both surface tension and density changes. Table 1 below is the summary of the above review.

Table 1. Summary of the review on Rayleigh-Bénard-Marangoni Convection

Ref & Author (Year)	Contributions	Key Findings	Limitations
Dubey *et al.* (2025)	Studied Rayleigh–Bénard–Marangoni convection in binary fluids with miscibility effects.	Miscibility alters oscillatory instability and transition thresholds.	Preprint without experimental validation.
Schindler *et al.* (2025)	Analyzed thermal boundary layer dynamics in turbulent liquid metal convection.	Fluid flow strongly influences boundary layer structure and heat transfer.	Focused only on turbulent regimes.
Song *et al.* (2024)	DNS of rapidly rotating Rayleigh–Bénard convection at high Rayleigh numbers.	Rotation modifies turbulence and heat transport scaling.	Excludes surface tension-driven convection.
Elbousefi *et al.* (2025)	Investigated Marangoni convection with deformable interfaces.	Interface deformation affects thermocapillary flow patterns.	Limited to confined geometries.
Yan *et al.* (2025)	Phase-field simulation of thermocapillary droplet migration.	Inclination and thermal gradients control droplet motion.	Focused on single-droplet systems.
Veena & Siddheshwar (2024)	Energy stability analysis of RBM convection in nanoliquids.	Nanoparticles modify stability and energy dissipation.	Mostly theoretical analysis.
Waris & Lappa (2024)	Thermographic study of topographically controlled RBM convection.	Surface topology alters convection onset and symmetry.	Complex temperature-dependent modeling.
Liapidevskii (2024)	Two-layer equilibrium model for miscible fluid flow.	Analytical insight into stratified fluid dynamics.	Simplified equilibrium assumptions.
Verma *et al.* (2024)	Studied light momentum interaction with layered fluids.	Optical forcing induces interfacial fluid motion.	Specialized experimental setup.
Huang *et al.* (2024)	Examined Faraday instabilities in three-layer fluids.	Multi-mode instabilities due to interface coupling.	Focused on vibration-induced effects.
Costa *et al.* (2025)	CFD study of multilayer cooling channels.	Multi-layer designs improve cooling efficiency.	Engineering-focused application.
Wang *et al.* (2024)	Heat transport analysis in two-layer convection systems.	Layer interactions affect heat transfer scaling.	Mostly numerical validation.

The research on fluid convection has reached new development stages which investigate how multilayer systems operate together with their interfacial coupling effects and their nonlinear instability properties during both buoyancy-driven and thermocapillary-dominated flow conditions. The implementation of high-resolution numerical simulations together with thermographic experiments has led to better insights about boundary layer behavior and suitable heat transport methods and interface behavior which occurs in systems with layered liquid materials. The research studies have explored various topics which include rotating convection and miscible and immiscible layered fluids and deformable interfaces and magnetic induction effects and optical momentum-induced flows to show how scientists are increasingly investigating multiphysics interactions inside complex fluid systems. The current computational methods directly numerical simulations and phase-field modelling and advanced CFD techniques enable researchers to study multilayered convection patterns. The existing system lacks a complete framework which can perform systematic studies of hybrid Rayleigh-Bénard-Marangoni interactions in multilayer systems that require dimensional analysis. This gap in research drives the need for our current study.

Background of The Study

Hybrid Marangoni-Bénard-Rayleigh convection refers to a situation where all three convection mechanisms - Marangoni, Bénard, and Rayleigh - interact and contribute to the fluid motion in a single system. This can occur in complex scenarios where multiple factors, such as temperature gradients, concentration gradients, and density differences, are simultaneously influencing the fluid flow. In such cases, the interplay of these mechanisms can lead to intricate and often unpredictable flow patterns as each of the following mechanisms can interact:

Marangoni Convection:

Marangoni convection, also referred to as surface-tension-driven convection, arises as a result of fluctuations in surface tension along a fluid's interface. Surface tension is the cohesive force that holds the molecules at the surface of a liquid together. When there are gradients in temperature or concentration at the interface, the surface tension can change, creating a force imbalance that drives fluid motion. This effect is particularly pronounced in liquids where temperature or concentration differences lead to varying degrees of surface tension.

For example, consider a liquid film with an initially uniform temperature. If one region is heated, its surface tension decreases, causing it to exert less resistance to the surrounding fluid. This leads to fluid flow from the cold to the hot region, amplifying the temperature difference. Similarly, if there is a concentration gradient along the interface (for instance, due to evaporation), the Marangoni effect can drive fluid motion.

Bénard Convection:

When a fluid layer is heated from below, a process known as Rayleigh-Bénard convection, also known as Benard convection, takes place. Due to buoyancy forces, the fluid close to the bottom warms up, becomes less dense, and rises. The fluid rises, cools, and gets denser, sinking back down as a result. Convection cells are established as a result of the rising and sinking fluid cycle that is created.

In Bénard convection, the Rayleigh number (Ra) is an important variable. It determines the beginning of convection and measures the proportion of buoyant forces to viscous forces. The fluid doesn't move if the Ra value falls below a threshold level. Convection cells begin to develop above this critical Ra, with warmer fluid ascending in the center and cooler fluid descending along the cell edges.

Rayleigh Convection:

Rayleigh convection, often referred to as Rayleigh-Taylor convection, is a phenomenon that occurs when a dense fluid is placed above a less dense fluid in a gravitational field. The denser fluid tends to sink while the lighter fluid rises, resulting in a mixing process. This type of convection is relevant in astrophysics, geophysics, and fluid dynamics. The Rayleigh number in this context characterizes the stability of the system. If the Rayleigh number exceeds a critical value, the initially stable interface between the two fluids becomes unstable, and convective motion sets in.

Marangoni-Bénard-Rayleigh convection is a phenomenon that occurs when a fluid is heated from below, causing variations in temperature that lead to fluid flow patterns. In addition to the Marangoni effect, which develops as a result of surface tension gradients at the fluid's interface, buoyant forces brought on by temperature variations also contribute to this convection. Marangoni-Bénard-Rayleigh convection has the following properties in the context of both 2D and 3D fluids:

2D Fluid

In a 2D fluid system, we consider a thin layer of fluid that is heated from below. The heat causes the fluid to expand, reducing its density and making it buoyant. The Marangoni effect is also at play due to variations in surface tension, which is typically influenced by the concentration of surface-active molecules or temperature gradients at the fluid's interface. The beginning of convection in a fluid layer is described by the dimensionless Rayleigh number (Ra). The Rayleigh-Bénard convection transition takes place in a 2D fluid when the critical Rayleigh number (Ra_c) is surpassed. Ra_c is dependent on the fluid properties, top and bottom temperature differences, and fluid layer dimensions.

The 2D fluid flow patterns in the convection cells are relatively simpler than in 3D. The convection cells can be visualized as long horizontal rolls that develop when the Rayleigh number surpasses the critical value. These rolls are aligned parallel to the temperature gradient and exchange heat and momentum between the hot rising fluid and the cooler descending fluid.

3D Fluid

In a 3D fluid system, the convection patterns become more complex due to the additional dimension. The heat from the bottom of the fluid layer induces vertical and horizontal fluid motions. In this case, convection cells are not just rolls, but they also include additional circulation patterns in the third dimension.

The transition to convection, characterized by the critical Rayleigh number (Ra_c), still occurs, but the patterns that emerge in the fluid are more intricate. The Marangoni effect and the complex interaction between buoyancy forces in the vertical and horizontal directions give rise to a variety of flow patterns, such as plumes, rolls, and vortices. Figure 1 represents the general model of 2D and 3D fluid system.

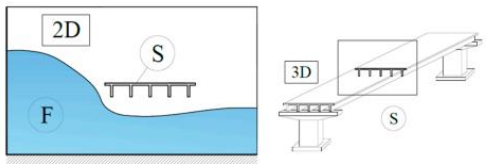


Figure 1. General model and multiscale formulation for the fluid and structural systems

Mathematical Modelling

In a hybrid scenario, the interactions between these mechanisms can lead to a wide range of flow patterns and behaviours that are challenging to predict analytically. Numerical simulations are often used to understand the combined effects of Marangoni, Bénard, and Rayleigh convection.

2D fluid system

In a 2D fluid layer, the Marangoni effect arises from surface tension gradients at the fluid's boundary. If there are temperature or concentration differences across the interface, the surface tension changes, inducing fluid motion. For instance, if a local region is heated, the lower surface tension in that area can lead to fluid flow from regions with higher surface tension. This can create fluid currents and circulation patterns within the 2D layer. Moreover, in a 2D fluid layer heated from below, the Bénard convection effect comes into play. Warm fluid near the bottom becomes buoyant and rises, while cooler fluid sinks. This creates convection cells where hot fluid rises in the center and descends along the cell boundaries. In a 2D system, these cells are elongated rolls aligned parallel to the temperature gradient. Furthermore, in a 2D fluid layer, the Rayleigh convection effect refers to instability caused by density differences due to temperature or concentration gradients. If a denser fluid rests above a less dense fluid, the interface can become unstable, leading to mixing and flow patterns. This phenomenon is relevant when discussing the interaction of temperature and density gradients.

Consider a fluid system with two layers. The rectangular cavity has the following dimensions: L x (H_1 + H_2). The thickness ratio between the layers is Hr = H_1/H_2, with the top fluid layer being H_1 and the bottom layer being H_2. The bottom of the system is uniformly heated from below at a heating rate of l°C/h. At a constant temperature Tc, the top wall is maintained. The two fluids must be totally immiscible, the interface must not deform, there must be two-dimensional convection, and the fluids must be incompressible using the Bossiness approximation.

The subsequent dimensionless Navier-Stokes and energy equations are expressed in the form of basic dependent variables, and they regulate the two-dimensional unsteady flows in each layer. The governing dimensionless equations for the two-layer fluid system are expressed as follows. The continuity equation is given by:

$$\Delta V_i = 0 \tag{1}$$

The momentum equation is written as

$$\partial \boldsymbol{V}_i / \partial t + \boldsymbol{V}_i \nabla \boldsymbol{V}_i = -C_i^{\rho} \nabla p_i + C_i^{\mu} \nabla^2 \boldsymbol{V}_i + C_i^{\alpha} \theta_i j \tag{2}$$

The energy equation is given by

$$\partial \theta_i / \partial t + V_i \nabla \theta_i = C_i^N \nabla^2 \theta_i \tag{3}$$

where i=1 stands for the liquid in the upper layer and i=2 for the liquid in the lower layer. The dimensionless speed is V_i= (u_i, v_i, 0), and the vertical unit vector J is pointed in the opposite direction as gravity. $\theta_i = (T_i - T_c)/\Delta T$, dimensionass temperature; and p_i, dimensionless pressure. The dimensionless coefficientsC_i^{ρ}, C_i^{μ}, C_i^{α}, and C_i^N represent the density ratio parameter, viscosity ratio parameter, buoyancy-related thermal expansion parameter, and thermal diffusivity ratio parameter, respectively, arising from the non-dimensionalization process. We use $H_2^2/\kappa_2, \kappa_2/H_2, H_2, \Delta T$ and $\rho_2 \kappa_2^2 / H_2^2$ as scales or time, velocity, length, temperature, and pressure, respectively, where H_2 is the thickness of the lower layer, K_2 is the thermal diffusivity of the lower layer, and ρ_2 is its density. Then, in the right-hand ide of these dimensionless equations, (1) - (3), the 'constants' are, respectively.

$$\begin{aligned} C_1^{\varphi} &= \rho_2/\rho_1 & C_1^{v} &= Pr\nu_1/\nu_2 \\ C_1^{\alpha} &= \alpha_1 g \Delta T H_2^3/\kappa_2^2 & C_1^{\kappa} &= \kappa_1/\kappa_2 \\ C_2^{\rho} &= 1 & C_2^{v} &= Pr \\ C_2^{a} &= \alpha_2 g \Delta T H_2^3/\kappa_2^2 & C_2^{\kappa} &= 1 \end{aligned} \tag{4}$$

The Prandtle number of liquids, Pr=v_2/k_2, density, kinematical viscosity, expansion coefficient, g, gravitational acceleration, T=T_h-T_c, external temperature differential between the lower and higher heating walls, and thermal diffusivity are all included in this equation.

The no-slip requirement is met on all borders. The continuity requirement is met for temperature, heat flux, tangential components of velocities, and stresses at the interface, where the normal components of velocities vanish. The lower wall, with temperature T_h, is heated from T_r to a higher temperature T= c+ΔT while the top wall is kept at a constant temperature T_c. Consider the opposite side walls to be adiabatic. It is presumable that the surface tension at the contact changes linearly with temperature, we have: $\sigma = \sigma_0 - \gamma(T - T_0)$, where T_0 is the reference temperature; and $\gamma = -\partial\sigma/\partial T$, this is the surface tension coefficient at different temperatures. The boundary conditions can therefore be stated as follows:

1. at the two vertical side-walls ($x = 0$ and $x = L/H_2$)

$$\begin{aligned} u_i &= v_i = 0 \\ \partial\theta_i/\partial x &= 0 \end{aligned} \tag{5}$$

2. at the horizontal walls: ($y = -1$ and $y = H_r$)

$$u_i = v_i = 0$$
$$\theta_2 = \text{ const } (y = -1)\ \theta_1 = 0 (y = H_t) \quad (6)$$

where 'const' is a constant which represents the heating rate. We take $c = 3600\kappa_2/(H_2^2\Delta T)$ in our numerical simulation for the heating rate of $1°\text{C/h}$, (3) at the interfaces: $(y = 0)$

$$u_1 = u_2$$
$$v_1 = v_2 = 0$$
$$\frac{\partial u_2}{\partial y} - \frac{\mu_1}{\mu_2}\frac{\partial u_1}{\partial y} = -Ma\frac{\partial \theta_2}{\partial x} \quad (7)$$
$$\frac{\lambda_1}{\lambda_2}\frac{\partial \theta_1}{\partial y} = \frac{\partial \theta_2}{\partial y}$$
$$\theta_1 = \theta_2$$

Equations (8)-(12) reflect the continuity of tangential velocity, kinematical condition, tangential stress balance, heat flow continuity, and temperature continuity, respectively. λ_i denotes thermal conductivity. Marangoni number is defined as $Ma = \gamma\Delta T H_2/\mu_2\kappa_2$.

Before the commencement of Rayleigh-Marangoni-Benard convection in the system, the initial temperature field is uniform, and the fluids are at rest.

Three Rayleigh numbers and three Marangoni numbers should be found in a system of two-layer fluids, where the total temperature of the system is 4.23°C calculated numerically, and 4.56°C measured in the experiment.

The temporal fluctuation of the largest non-dimensional stream function, max. Under a temperature difference (ΔTc), the value of Ψmax is almost 0, which denotes that the fluid is still at rest, according to a linear change of temperature difference with time. The value of max increases quickly when the temperature difference (ΔT) keeps growing very little. This corresponds to the situation where the convective flow is gradually produced in the system of two-layer liquids. The present research uses the nonlinear evolution of Ψmax to establish numerically the crucial parameters corresponding to the time at point 'c' for the beginning of Rayleigh-Marangoni-B4nard convection. These three convection processes can interact hybridly in a 2D fluid layer to produce intricate flow patterns. Here's one that may happen:

Imagine a 2D fluid layer with a temperature gradient from bottom to top. This establishes a Bénard convection setup with rolls aligned along the temperature gradient. If there are concentration differences due to, for example, evaporation, the Marangoni effect can be triggered. This can modify the surface tension, influencing the Bénard convection cells. Fluid flow driven by Marangoni forces can superimpose onto the existing Bénard convection patterns, altering their behaviour. If there are density variations due to temperature or concentration gradients, Rayleigh convection can occur. This introduces instability at the interface, leading to mixing and fluid motion. The Rayleigh convection cells can interact with both Bénard and Marangoni flows, further complicating the fluid dynamics.

Thus this provide more accurate solutions for problems with strong gradients or singularities. It offers flexibility in selecting the approximation functions (basis functions) and allows for higher-order approximations. It can handle problems with irregular or non-uniform meshes. It can handle problems with mixed boundary conditions more effectively.

3D fluid system

Hybrid Marangoni - Bénard - Rayleigh convection in a 3D fluid layer refers to the simultaneous interaction of these three convection mechanisms within a three-dimensional fluid domain. This complex scenario results in intricate and often unpredictable flow patterns due to the interplay of temperature, concentration, and density gradients. Here's an explanation of how these mechanisms interact in a 3D fluid layer:

In a 3D fluid layer, the Marangoni effect arises from surface tension gradients at the fluid interface caused by temperature or concentration differences. Fluid flows can be driven from regions of lower surface tension to those of greater surface tension when there are fluctuations in surface tension. At the fluid interface, this action is very potent and can cause intricate fluid motion patterns. Bouyancy-driven fluid motion causes Bénard convection to begin in a 3D fluid layer that has been heated from below. Warm fluid near the bottom becomes buoyant and rises, while cooler fluid descends. This leads to the formation of convection cells where hot fluid rises in the center and cooler fluid sinks along the cell boundaries. In a 3D system, these cells can extend both vertically and horizontally. Rayleigh convection in a 3D fluid layer refers to instability arising from density differences due to temperature or concentration gradients. If denser fluid is positioned above less dense fluid, the interface can become unstable, leading to mixing and complex flow patterns. This phenomenon is relevant when considering the interaction between temperature and density gradients.

LSFEM stands for 'Least Squares Finite Element Method.' It is a numerical technique used for solving partial differential equations (PDEs) that arise in various fields of science and engineering, such as physics, fluid dynamics, structural analysis, and more. In LSFEM, the main idea is to find an approximation of the solution to the PDE by

minimizing the residuals over the entire domain using a least squares criterion. LSFEM has applications in a wide range of fields where PDEs need to be solved accurately and efficiently. These include heat transfer, fluid dynamics, structural mechanics, electromagnetics, and more. It's worth noting that while LSFEM offers certain advantages over traditional FEM, the choice of which method to use depends on the specific characteristics of the problem and the computational resources available.

Using the LSFEM, the first order system of equations is solved. The number of equations and the number of unknowns do not need to be the same because the LSFEM is flexible. So, the numerical solution does not take into account the dummy variables. The LSFEM is used to find the solution to the first-order system with fifteen equations and eleven unknowns. Considered is the vector form of these equations,

$$\mathrm{A}_1\frac{\partial \mathrm{q}}{\partial x}+\mathrm{A}_2\frac{\partial \mathrm{q}}{\partial y}+\mathrm{A}_3\frac{\partial \mathrm{q}}{\partial z}+\mathrm{S}=0, \tag{8}$$

Where A_1, A_2 and A_3 are coefficient matrices corresponding to spatial derivatives. When each item in the right-side vector S represents a mathematical problem with eleven dependent variables, i.e.,

$$s_i = s_i(q_1, q_2, \cdots, q_{11})\ i = 1,2,\cdots,15 \tag{9}$$

Where q represents the vector of unknown variables $q_j, j = 1,\cdots,11$. Newton's method linearizes the nonlinear terms in a particular way:

$$s_i^{m+1} = s_i^m + \sum_{j=1}^{11}\left(\frac{\partial s_i}{\partial q_j}\right)^m \Delta q_j, \tag{10}$$

where m+1 represents the current step in the Newton's technique, and the superscript m stands for the step that came before $\Delta q_j = q_j^{m+1} - q_j^m$ is the increment of the flow variables in each Newton's iteration. We manipulate the equations to create a new set of vector equations that are suitable for finite element discretization.

$$\begin{aligned}&\mathrm{A}_o^m\Delta\mathrm{q}+\mathrm{A}_1^m\frac{\partial \Delta\mathrm{q}}{\partial x}+\mathrm{A}_1^m\frac{\partial \mathrm{q}^m}{\partial x}+\mathrm{A}_2^m\frac{\partial \Delta\mathrm{q}}{\partial y}+\\&\mathrm{A}_2^m\frac{\partial \mathrm{q}^m}{\partial y}+\mathrm{A}_3^m\frac{\partial \Delta\mathrm{q}}{\partial z}+\mathrm{A}_3^m\frac{\partial \mathrm{q}^m}{\partial z}+\mathrm{S}^m=0(72)\end{aligned} \tag{11}$$

The equations that govern are then transformed into the subsequent operator form to continue:

$$L\Delta q = f, \tag{12}$$

where the definition of the linear operator L is

$$\mathrm{L}=\mathrm{A}_o^m+\mathrm{A}_1^m\frac{\partial}{\partial x}+\mathrm{A}_2^m\frac{\partial}{\partial y}+\mathrm{A}_3^m\frac{\partial}{\partial z}. \tag{13}$$

The vector on the right is

$$\mathrm{f}=-\mathrm{A}_1^m\frac{\partial \mathrm{q}^m}{\partial x}-\mathrm{A}_2^m\frac{\partial \mathrm{q}^m}{\partial y}-\mathrm{A}_3^m\frac{\partial \mathrm{q}^m}{\partial z}-\mathrm{S}^m. \tag{14}$$

Then, for admissible $\Delta\mathrm{q}$, we indicate the least-squares functional of the residual $\mathrm{R}=\mathrm{L}\Delta\mathrm{q}-\mathrm{f}$ as

$$J(\Delta\mathrm{q})=\int_\Omega \mathrm{R}^T\cdot\mathrm{R}d\Omega. \tag{15}$$

The result is obtained by minimising the least-squares functional $J(\Delta\mathrm{q})$ with respect to Δq.

$$\delta J(\Delta\mathrm{q})=0. \tag{16}$$

Which is,

$$\int_\Omega (\mathrm{L}\delta\Delta\mathrm{q})^T\cdot(\mathrm{L}\Delta\mathrm{q}-\mathrm{f})d\Omega=0, \tag{17}$$

where δ represents the deviation of the function. Let $\delta\Delta\mathrm{q}=\mathrm{v}$, and (78) was represented as

$$\int_\Omega (\mathrm{Lv})^T(\mathrm{L}\Delta\mathrm{q})d\Omega=\int_\Omega (\mathrm{Lv})^T\mathrm{f}d\Omega. \tag{18}$$

where Ω denotes the computational domain, L represents the linearized differential operator, v is the test (weighting) function, q is the state vector of perturbation variables, and f represents the source vector.

The computational domain is divided into N_c elements in order to use the finite element approach and the introduction of the element shape functions Φ_i. Every element's discretized solution, $\Delta\mathrm{q}_h^{\mathrm{f}}(t,x,y,z)$ can be stated as

$$\Delta\mathrm{q}_h^{\epsilon}(t,x,y,z)=\sum_{i=1}^{N_n}\Phi_i(x,y,z)(\Delta\mathrm{Q}_i(t))^e, \tag{19}$$

In which $(\Delta\mathrm{Q_i}(t))^e$ represents the nodal values of $\Delta\mathrm{q}$ and N_n is the number of nodes for each component. It is decided to use test function v as

$$\mathrm{v}(x,y,z)=\Phi_i(x,y,z)\mathrm{I}, \tag{20}$$

where I represent the identity matrix. When (80) and (81) are substituted into (79), the linear algebraic calculation results.

$$\mathrm{K}^m\Delta\mathrm{Q}=\mathrm{F}^m, \tag{21}$$

where ΔQ represents the global nodal values of $\Delta q(x, y)$, as well as the final global matrix is

$$K^m = \sum_{e=1}^{N_e} (K^m)^e \quad (22)$$

In other words, the element matrix $(K^m)^\epsilon$ is constructed from the global matrix K^m, which can be described as

$$\left(K_{ij}^m\right)^e = \int_{\Omega_e} (L\Phi_i)^T \cdot \left(L\Phi_j\right) d\Omega. \quad (23)$$

Finally, the right-side element vector F^m is constructed through the element vector $(F_i^m)^e$, which is provided as

$$(F_i^m)^e = \int_{\Omega_e} (L\Phi_i)^T \cdot f d\Omega \quad (24)$$

The matrix is symmetric, which is a key aspect of the least-squares finite element approach. Additionally, the global matrix is definitively positive for as long as the solution is valid.

The coefficient matrix is inverted using the JCG technique. The technique is a simple and effective way to invert a symmetric positive-definite matrix. The numerical convergence of the JCG technique is assured as long as the solution exists. The preconditioned global matrix is free of fill-in because the Jacobi preconditioning process only modifies the global matrix's diagonal terms, and the entire process can be carried out element by element without the need to store the global matrix, making fine-grain parallelization simple. This benefit of the LSFEM is, in our opinion, particularly alluring for calculations on a large scale.

An incompressible fluid can naturally convect due to buoyancy forces brought on by temperature gradients and thermocapillary forces brought on by surface tension gradients. A temperature gradient is produced across the plates when both horizontal plates with a thin fluid layer placed among them are heated over underneath. Circular convection cells form at the critical Rayleigh number; the hot fluid at the bottom starts to ascend while the cooler fluid near the top starts to sink. This kind of ow known as the Rayleigh-Benard issue is mostly driven by buoyancy. The effects of surface tension caused by temperature variations on the free surface become significant if the plate is detached from the top surface. For this classic Rayleigh-Benard-Marangoni issue, the dominating forces driving the flow are now provided by both buoyancy and thermocapillary effects.

We take into account the Navier-Stokes calculations linked with the heat transfer (energy) calculation's description of the transient flow of viscous incompressible fluid. We restrict the analysis to two-dimensional flows with a non-deforming free surface in this instance. The Rayleigh-Benard-Marangoni flows are described by dimensionless equations that

$$\begin{aligned} \frac{\partial u}{\partial t} + u \cdot \nabla u - \Delta u + \nabla p &= -\frac{R_r}{P_r} g && \text{in } \Omega \\ \nabla \cdot u &= 0 && \text{in } \Omega \\ \frac{\partial I}{\partial t} + u \cdot \nabla 1 - \frac{1}{P_r}\nabla^2 I &= 0 && \text{in } \Omega \end{aligned}$$

where I is the temperature, p is the amount of pressure, and u is the speed. The Rayleigh number is $R_{is} = \frac{3\Delta T_q L^{-1}}{\text{is}}$. The Prandtl number is $P_r = \frac{L}{a}$. The thermal coefficient is written as β. ΔI represent the difference in temperature for moves with heated or cooled walls, and g represents the gravity vector. L stands for the flow's characteristic length scale, v for kinematic viscosity, and a for thematic diffusivity.

The following are the boundary conditions: $u = u_w$ (no slip) on $\partial\Omega_1$. $I = I_1(x, y)$ (isothermal boundary) or $\frac{\partial T}{M} = 0$ (adiabatic boundary) on $\partial\Omega_1$. where $\partial\Omega_1$ is the part of the boundary which is not a free surface. On the free surface $\partial\Omega_2$, the shear stress is equal to the gradient in the surface tension σ. Let us presume that σ differs linearly with I. so $o_Y = \frac{\partial J}{gT}$ is a constant for a given fluid. The non-dimensional boundary condition on ρ is the density. A coupled system of formulas consisting of (1), (2) and (3) must be addressed for velocity, pressure, and temperature.

The Navier-Stokes equations are solved first in each time step of the current algorithm's decoupled scheme, which causes the temperature to be delayed in the forcing term. Then, using the velocities as an input, the temperature is computed. In order to impose the incompressibility condition, the finite element flow formulation uses a penalty Galerkin technique, while the heat equation makes use of a Galerkin strategy.

Introducing a finite element discretization and basis on Ω_{h_h} the variational boundary value problem reduces to find $u_h \in V^h$ satisfying the initial condition with $u_h = u_w$ on $\partial\Omega_1$ such that

$$= \int_{\Omega_h} \frac{Ru}{P_r} I \, g \cdot v_h dx \quad \text{for all } v_h \in V^h$$

Where I denotes reduced numerical integration. This leads to the following non-linear semi discrete system of ordinary differential equations

$$\mathrm{M}\frac{d\mathrm{u}^*}{dt} + \mathrm{Au}^* + \mathrm{C}(\mathrm{u}^*) + \frac{1}{\epsilon}\mathrm{Bu}^* = \mathrm{F}$$

Where $\mathrm{C}(\mathrm{u}^*)$denotes the nonlinear convection term resulting from the discretized advection operator.

This uses a CrankNicolson technique for implicit integration and is linearized by iterative approximations. Using a frontal solver, the linear systems' solution is discovered.

To identify approximations of solutions for the transport issue associated with (3). We employ a conventional finite element formulation with Galerkin. The diffusion element can be partially integrated in a typical residual formulation to get a week variational statement. applying the Gauss Divergent Theorem after that. It can build a semidiscrete Galerkin finite element technique by presenting a spatial discretization and a suitable finite clement space for the admissible functions, supposing that convective and diffusive effects are of the same order. The finite element difficult is to find $T_h \in {H_0}^h$ addressing the initial requirement so that

$$\int_{\Omega_s}\left(\frac{\partial I_{h_1}}{\partial t}\omega_{h_1} + \mathbf{u}\cdot\nabla I_{h_1}\omega_{h_1} + \frac{1}{P_r}\nabla I_{h_1}\cdot\nabla\omega_{h_1}\right)dx = 0$$

for all $\omega_h \in {H_0}^h$. In this the nodal vector T, the outcome of the semi-discrete ODE system possesses the following format as

$$\mathrm{M}\frac{d\mathrm{T}}{dt} + \mathrm{B(u)T} + \mathrm{DT} = 0$$

Where $B(u)$ represents the convection matrix associated with the velocity field u.

Using a Crank-Nicolson technique, we implicitly integrate the ODE system. We use a frontal solver to solve a linear problem at each timestep.

Control is the process of getting a set of variables to adhere to a predetermined value or reference value. In closed-loop method control, the controlled variable is measured, and a feedback signal is used to compare the result to a reference value. The controller receives data from some type of output sensor, which it uses as an input to determine how distant the result deviates from the reference value. This data is used by the controller to fix the output error.

The Proportional-integral-Differential (PID) control loop, a three-term control system, is among those most frequently utilized closed-loop controller techniques. PID controllers' widespread use may be due to both their strong performance under a wide range of operating situations and their functional simplicity. The objective of PID control methods is to minimize overshoot while guiding the output together a smooth curve (versus time) to the set point. Overshoot is the degree that the system's result differs from the target response. Step size selection may be seen as an automated control issue with a PID controller, according to Hairet and Wanner

$$\Delta t_{n+1} = \left(\frac{e_{n-1}}{e_n}\right)^{k_n}\left(\frac{tol}{e_n}\right)^{k_n}\left(\frac{e_{n-1}^2}{e_n e_n}\right)^{k_D}\Delta t_n.$$

wherever tol is about input tolerance, e_n is an estimation of how the amounts of interest have changed over time Δt_n, and k_p, k_l and k_D are the PID parameters.

The proposed evolution estimate has been contrasted to the verified accuracy need so as to establish the new duration of the step. The controller tries to choose the step size such that $\mathrm{f_n}$ follows a smooth curve and approaches the input tolerance, tol, as closely as feasible. The measurement of the interest quantities' change across a timestep. The definition of $\mathrm{c_n}$.

$$e_n = \max(e_{11}, e_7)$$

Where

$$c_u = \frac{\dot{\epsilon}_u}{tol_u} \text{ with } \tilde{e}_u = \frac{\|\mathrm{u}^*_{m+1} - \mathrm{u}^*_m\|}{|\mathrm{u}^*_{m+1}|}$$
$$c_u = \frac{\hat{e}_T}{t_1} \text{ with } \hat{e}_T = \frac{\|\mathrm{T}_{m+1} - \mathrm{T}_m\|}{\|\mathrm{T}_{m+1}\|}$$

Here e_n and e_T are the normalized variations in nodal velocity and the temperatures, accordingly and ||.|| denotes the Euclidern norm. The related user-supplied limits are shown as tol_u and tol_T. We provide timestep limits. $(\Delta t)_{\mathrm{man}}$ as well as $(\Delta t)_{\mathrm{max}}$, to take the anti_windup effect into account.

The temperatures are used as an input in the forcing term at each timestep to determine the velocities. then the new velocities are used to calculate the temperatures. (9) provides the new timestep size. The updated temperatures and velocities are used to compute the new solutions. A timestep is rejected if it returns an undesirable value for _n. Following that, a timestep dimension is used to reprise the step that has been adjusted dependent on how much the crer differs from the tolerance. The number of rejections, however, turns out to be quite low in our numerical studies, resulting in a timestep sequence that is smooth.

If the nonlinear system's iterative sequence is convergent slowly in our algorithm. Also rejected is the timestep.

In a 3D fluid layer, the hybrid interaction of Marangoni, Bénard, and Rayleigh convection mechanisms can lead to intricate flow patterns that are challenging to predict. Imagine a 3D fluid layer with a combination of temperature and concentration gradients, such as a heated fluid layer with varying concentrations. The Marangoni effect can be triggered due to concentration differences along with the temperature gradient. Variations in surface tension at the interface can drive complex fluid flows that interact with the existing Bénard convection cells. The Bénard convection cells, driven by buoyancy forces, can interact with the Marangoni flows and modify their behavior. The presence of multiple convective motions can lead to the emergence of new flow patterns and vortices. Rayleigh Interaction: If there are density differences due to temperature or concentration variations, Rayleigh convection can further complicate the flow. The instability at the interface can disrupt existing convection patterns and introduce additional mixing and motion.

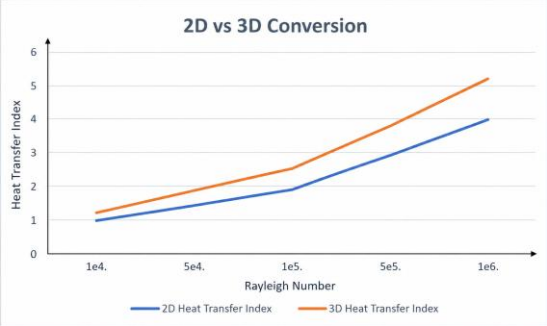


Figure 2. Comparison of Convection Behaviour in 2D and 3D Systems

The heat transfer index changes as shown in the Figure 2 as the Rayleigh number increases. As the Rayleigh number increases from 1×10 to 1012, both the 2D and 3D heat transfer indices increase gradually. Both the 2D and 3D heat transfer indices increase steadily with the increase of Rayleigh number from 1×10^4 to 1×10^6, representing greater natural convection heat transfer. The 3D heat transfer index is always higher than the 2D index at all Rayleigh numbers, indicating the higher thermal performance predicted by the 3D model. The difference between the two models becomes more prominent at higher Rayleigh numbers indicating that the three-dimensional flow effects have a significant contribution on heat transfer enhancement. The overall results indicate that the 3D model gives a better representation of the convective heat transfer behaviour than the 2D model.

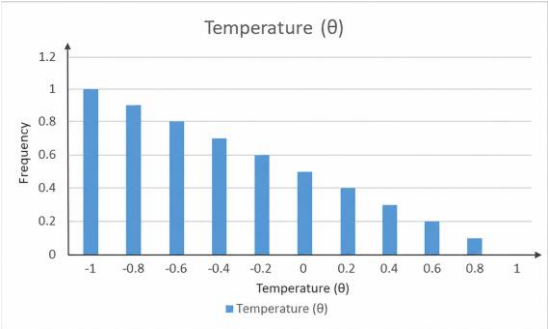


Figure 3. Temperature Profile across Two Layers

The figure 3 shows the variation of dimensionless temperature along the vertical direction across the two-layer fluid system. The temperature decreases monotonically from the heated lower boundary to the cooled upper boundary, indicating a stable thermal gradient. A continuous temperature profile is observed at the interface, satisfying interfacial thermal continuity conditions. The slope change across the interface reflects differences in thermal properties between the two fluid layers. This profile validates the imposed boundary conditions and demonstrates the thermal coupling behaviour in multilayer convection systems.

Summary

In summary, hybrid Marangoni-Bénard-Rayleigh convection in a 3D fluid layer involves the simultaneous interaction of these three convection mechanisms: Marangoni effects due to surface tension gradients, Bénard convection driven by buoyancy forces, and Rayleigh convection due to density differences. The resulting flow patterns are highly intricate and depend on the interplay of these mechanisms, making this scenario challenging to analyze and understand fully. Numerical simulations and experimental studies are often employed to gain insights into the complex behaviors that arise in such systems. Table 2 below is the summary of the above study.

Table 2. Summary of the review about 2D & 3D fluid systems

Aspect	2D Fluid Surfaces	3D Fluid Surfaces
Dimensionality	Confined to two dimensions (x-y plane)	Extends in three dimensions (x-y-z volume)
Flow Patterns	Horizontal rolls or cells	Three-dimensional, complex flow patterns
Driving Mechanisms	Buoyancy-driven and surface tension effects	Interaction of buoyancy, surface tension, and possibly density effects
Flow Dominance	Horizontal flow dominates	Flow in all three dimensions
Primary Driving Force	Temperature difference	Surface tension gradient and buoyancy forces
Spatial Extent of Patterns	Extends horizontally and vertically	Three-dimensional throughout the fluid volume
Temperature Distribution	Vertical temperature variations	Temperature variations in both vertical and horizontal directions
Key Parameters	Rayleigh number (Ra)	Marangoni number (Ma), Prandtl number (Pr), and possibly Lewis number (Le)
Pattern Formation Mechanism	Buoyancy-driven instability	Surface tension gradient instability
Instabilities	Buoyancy-driven instability	Surface tension gradient instability
Complexity of Flow Patterns	Relatively simpler	Highly complex, intricate flow patterns
Application Focus	Heat transfer, fluid dynamics	Materials processing, microfluidics, fluid behavior studies
Spatial Distribution of Patterns	Regular cells or rolls	Evolving, interacting flow structures
Spatial Scale of Patterns	On the order of fluid depth	May span a range of scales
Experimental Observations	Often visible with smoke or dye	May require advanced visualization techniques
Numerical Simulations	Relatively computationally efficient	More computationally demanding
Techniques for Study	Flow visualization, infrared imaging	Numerical simulations, experimental observations
Effect of Surface Tension	Less pronounced in 2D systems	Can play a significant role in 3D systems
Effect of Density Differences	Less pronounced in 2D systems	Can introduce additional complexity in 3D systems

Rayleigh - Bénard - Marangoni convection processes exhibit distinct behaviors on 2D and 3D fluid surfaces. In 2D fluid layers, such as thin films, the dominant convection patterns are often characterized by horizontal rolls or cells driven by buoyancy forces resulting from temperature differences. Marangoni convection can contribute surface flow patterns due to surface tension gradients caused by variations in temperature or concentration. In contrast, 3D fluid volumes introduce an additional dimension, leading to more complex and three-dimensional flow patterns. Buoyancy-driven Bénard convection still plays a significant role, but now extends vertically and horizontally. The Marangoni effect in 3D can induce intricate surface flows due to surface tension gradients, while the interaction of temperature, concentration, and possibly density differences can create highly intricate and evolving flow structures throughout the fluid volume. Overall, the distinction lies in the complexity and spatial extent of flow patterns, with 2D systems exhibiting simpler horizontal rolls and 3D systems displaying intricate and evolving three - dimensional flows.

Conclusions

In conclusion, this comprehensive review paper has explored the intricate dynamics of Rayleigh-Bénard-Marangoni convection in the context of both 2D and 3D fluid surfaces using mathematical modeling techniques. Through an in-depth analysis of the fundamental mechanisms driving each convection type and their interplay, this review has shed light on the distinct characteristics of convection patterns and flow behaviors in these dimensions. The mathematical models discussed here serve as valuable tools for simulating and understanding the complex phenomena associated with convection processes. By elucidating the impacts of key parameters, such as Rayleigh and Marangoni numbers, on the observed behaviours, this study has provided insights into the underlying physics and behaviours of convection in various scenarios. This review paves the way for further research and applications in heat transfer, fluid dynamics, and materials processing, enabling a more profound comprehension of convection phenomena on different fluid surfaces.

Funding

The authors state that this work has not received any funding.

Author Contributions

Conceptualization: K.V., G.B.C.M.; Methodology: K.V.; Formal Analysis: K.V., G.B.C.M.; Investigation: K.V., G.B.C.M.; Writing - Original Draft: K.V.; Writing - Review & Editing: K.V., G.B.C.M.; Supervision: G.B.C.M. All authors have read and agreed to the published version of the manuscript.

Ethics Statement

Ethical approval was not required for this study because it is a review of previously published literature on Rayleigh-Bénard-Marangoni convection and mathematical modelling. The study did not involve human participants, animals, biological materials, or the collection of personal or identifiable data.

Declaration of Generative AI Use

The authors declare that no Generative Artificial Intelligence (Generative AI) tools were used in the preparation, writing, or revision of this manuscript.

Conflict of Interest

They author declare that have no conflict of interest

Data Availability Statement

No new datasets were generated or analyzed during this study. The information discussed in this review is based on previously published literature, which is cited in the manuscript.

Acknowledgement

The authors would like to thank the Deanship of Vardhaman College of Engineering for supporting this work.

References

Bombe, D., Kumar, R., Nandi, S. K., & Agrawal, A. (2024). Semi-analytical formulation for single-track laser powder-bed fusion process to estimate melt-pool characteristics considering fluid-flow and Marangoni effect. *International Journal on Interactive Design and Manufacturing (IJIDeM)*, *18*(7), 5121-5137. https://doi.org/10.1007/s12008-023-01593-1

Botarelli, T., Fanfani, M., Nesi, P., & Pinelli, L. (2025). Using physics-informed neural networks for solving Navier-Stokes equations in fluid dynamic complex scenarios. *Engineering Applications of Artificial Intelligence*, *148*, Article 110347. https://doi.org/10.1016/j.engappai.2025.110347

Costa, S., Capela, P., Hassui, A., Ribeiro, J., Pereira, M., & Soares, D. (2025). CFD analysis of multi-layer cooling channels in three-dimensionally structured grinding wheels. *Applied Thermal Engineering*, *279*, Article 127633. https://doi.org/10.1016/j.applthermaleng.2025.127633

Dubey, A., Mishra, S., Diwakar, S. V., & Amiroudine, S. (2025). Rayleigh - Bénard - Marangoni convection in binary fluids - Effect of miscibility on oscillatory mode [Preprint]. arXiv. https://doi.org/10.48550/arXiv.2504.10324

Elbousefi, B., Schupbach, W., & Premnath, K. N. (2025). Marangoni convection of self-rewetting fluid layers with a deformable interface in a square enclosure and driven by imposed nonuniform heat energy fluxes. *Energies*, *18*(13), 3563. https://doi.org/10.3390/en18133563

Huang, Y. F., Zhuo, R. L., Yang, J. C., & Ni, M. J. (2024). Interface coupling effect and multi-mode Faraday instabilities in a three-layer fluid system. *Journal of Fluid Mechanics*, *982*, A8. https://doi.org/10.1017/jfm.2024.43

Jiang, H., Liao, W., & Chen, E. (2024). Bénard-Marangoni convection in an open cavity with liquids at low Prandtl numbers. *Symmetry*, *16*(7), Article 844. https://doi.org/10.3390/sym16070844

Liapidevskii, V. Y. (2024). Two-layer equilibrium model of miscible inhomogeneous fluid flow. *Fluid Dynamics*, *59*(4), 709-722. https://doi.org/10.1134/S0015462824603395

Maharani, N. S., Karim, S., Liliawati, W., & Sandion, A. (2024). Development of website media based on Google Sites to improve students' conceptual understanding on dynamic fluid materials. *Mimbar Pendidikan*, *9*(2), 72-86. https://doi.org/10.17509/mimbardik.v9i2.75165

Rahman, M. S. (2024). Computational fluid dynamics for predicting and controlling fluid flow in industrial equipment. *European Journal of Advances in Engineering and Technology*, *11*(9), 1-9.

Saini, M., Sanjay, V., Saade, Y., Lohse, D., & Popinet, S. (2025). *Implementation of integral surface tension formulations in a volume of fluid framework and their applications to Marangoni flows* [Preprint]. arXiv. https://doi.org/10.48550/arXiv.2502.02712

Sari, I., Wu, M., Ludwig, A., & Kharicha, A. (2024). Effect of Marangoni flow during the solidification of a Fe-0.82wt.%C steel alloy. *Journal of Physics: Conference Series*, *2766*(1), Article 012198. https://doi.org/10.1088/1742-6596/2766/1/012198

Schindler, F., Kim, N., Vogt, T., & Eckert, S. (2025). Impact of fluid flow on the thermal boundary layer dynamics in turbulent liquid metal Rayleigh-Bénard convection. *International Journal of Heat and Mass Transfer*, *247*, Article 127129. https://doi.org/10.1016/j.ijheatmasstransfer.2025.127129

Song, J., Shishkina, O., & Zhu, X. (2024). Direct numerical simulations of rapidly rotating Rayleigh-Bénard convection with Rayleigh number up to 5×10^{13}. *Journal of Fluid Mechanics*, *989*, A3.

Umavathi, J. C., Buonomo, B., Manca, O., & Sheremet, M. A. (2025). MHD couple stress boundary-layer flow with heat and mass transfer under thermal radiation and Marangoni effect: A numerical study. *Case Studies in Thermal Engineering*, *71*, Article 106159. https://doi.org/10.1016/j.csite.2025.106159

Veena, B. N., & Siddheshwar, P. G. (2024). Energy stability analysis of Rayleigh-Bénard-Marangoni convection in homogeneous and heterogeneous nanoliquids. *Journal of Nanofluids*, *13*(6), 1177-1191. https://doi.org/10.1166/jon.2024.2203

Verma, G., Kumar, A., Soni, S., Yadav, K., & Li, W. (2024). Probing interplay of light momentum and fluid mechanics in two-layer liquids. *Physical Review Fluids*, *9*(3), Article 034801. https://doi.org/10.1103/PhysRevFluids.9.034801

Wang, M., Chen, X. Y., Wang, W., & Wei, P. (2023). Heat transport and flow structure in thermal convection with two liquid layers. *Journal of Fluid Mechanics*, *978*

Waris, W., & Lappa, M. (2024). Thermographic analysis of topographically controlled Marangoni-Rayleigh-Bénard convection in a fluid with temperature-dependent properties. *International Journal of Thermal Sciences*, *196*, Article 108718. https://doi.org/10.1016/j.ijthermalsci.2023.108718

Yan, H., Wang, L., Huang, J., & Yu, Y. (2025). Thermocapillary migration of a self-rewetting droplet on an inclined surface: A phase-field simulation. *Applied Thermal Engineering*, *263*, Article 125345. https://doi.org/10.1016/j.applthermaleng.2024.125345